

# *ESO observing programme SHARKS: Southern H-ATLAS Regions K<sub>s</sub>-band Survey (198.A-2006, PI. H. Dannerbauer)*

## **Abstract**

We describe the first data release from the Southern H-ATLAS Regions K<sub>s</sub>-band Survey (SHARKS-DR1). SHARKS is a deep K<sub>s</sub>-band survey of  $\sim 300$  square degrees covering large parts of the South Galactic Plane (SGP), GAMA-12h (G12) and GAMA-15h (G15) fields from the H-ATLAS survey, the largest Herschel program. These regions are covered by several optical and near-infrared surveys, including VIKING, HSC and DES, among others, as well as by the future LSST and Euclid. Using the K<sub>s</sub>-filter, observations have been conducted with the wide-field VIRCAM imager at the VISTA telescope. The project was granted 1200 hours of observing time under the ESO programme 198.A-2006. We aim at reaching a  $5\sigma$  magnitude limit of  $K_s \sim 22.7$  mag (AB), for example, to match  $\sim 90\%$  of the H-ATLAS sources up to redshift 3. SHARKS-DR1 is the first public data release of the ESO public survey SHARKS, consisting of calibrated K<sub>s</sub>-band images and source catalogues for  $\sim 20$  square degrees divided in 10 mosaics of  $\sim 2$  square degrees each. The ten mosaics are distributed as following: four contiguous mosaics in the SGP-E region, and two non-overlapping mosaics in each of the SGP-W, G15 and G12 fields. The mean depth reaches the expected depth at  $5\sigma$  of  $K_s \sim 22.7$  (AB) with a mean seeing of  $\sim 1''$ . SHARKS-DR1 has been produced in collaboration between the Instituto de Astrofísica de Canarias (IAC) and the Wide-Field Astronomy Unit (WFAU) at the Royal Observatory of Edinburgh. The data can be found at the ESO archive and also at:

<http://research.iac.es/proyecto/sharks/pages/en/data-releases/dr1.php>

## **Overview of Observations**

SHARKS-DR1 data comprises deep VISTA K<sub>s</sub>-band<sup>1</sup> observations of ten mosaics of  $\sim 2$  square degrees each. These are two mosaics each in the G12, G15 and in the western SGP (SGP-W) field, and four contiguous pointings in the eastern SGP field (SGP-E).

Each mosaic consists of the co-addition of at least seven VISTA tiles (seven OBs respectively visits of  $\sim 55$  minutes), and those images from adjacent tiles that overlap with the given mosaic (reaching full depth up to the edges).

Each tile (visit) follows the default VISTA survey strategy. It is formed by six stacked pawprints, shifted by half of a detector in the Y-direction, and 0.9 of a detector in the X-direction. Each stacked pawprint is made of six single-epoch (normal) images of ten seconds of effective exposure time each (average of  $6 \times 10$  second images), with a small random jitter pattern so that bad pixels or columns appear in different parts of the sky in each normal.

---

<sup>1</sup> <http://casu.ast.cam.ac.uk/surveys-projects/vista/technical/filter-set>

SHARKS-DR1 contains observations taken between 3 March 2017 and 18 January 2019 at 141 distinct nights. The survey strategy aims to complete each mosaic before moving to another, therefore the epoch difference within a mosaic is, in general, around a month. In Fig. 1 we show the distribution of epochs given by the modified julian day. The mean epoch is 58237 (29th of April 2018) in the G12, 57910 (6th of June 2017) in the G15, 58155 (6th of February 2018) in the SGP-W and 58389 (28th of September 2018) in the SGP-E field.

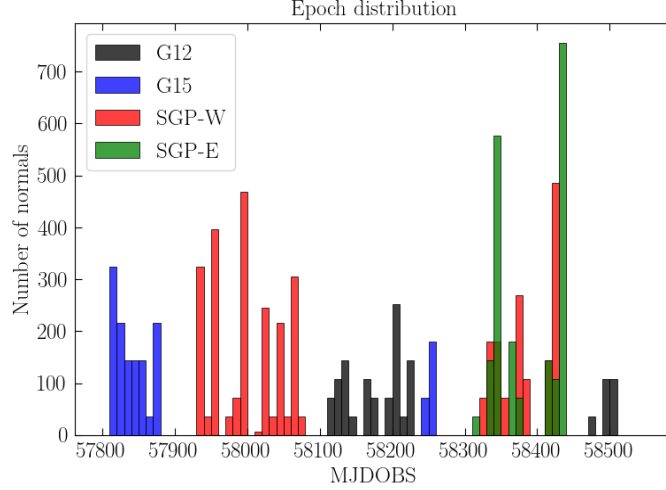


Figure 1: Epoch distribution for all normals that input the DR1 data, for the four SHARKS fields separately.

The required sky conditions for the stacked pawprints are: seeing  $< 1.2''$  in the SGP field and seeing  $< 1.0''$  in the GAMA fields, airmass  $< 1.7$  and clear weather conditions. If only one of these conditions are surpassed by less than 20%, we still keep the image as good. In other cases, observations are given a bad grade (esoGrade=C) and are sent back to the VISTA observing queue. Currently, grade C images are nonetheless archived and used to fill-up to the edges if it is adjacent to the mosaic footprint. Since we observe in the  $K_s$ -band, we do not have moon restrictions.

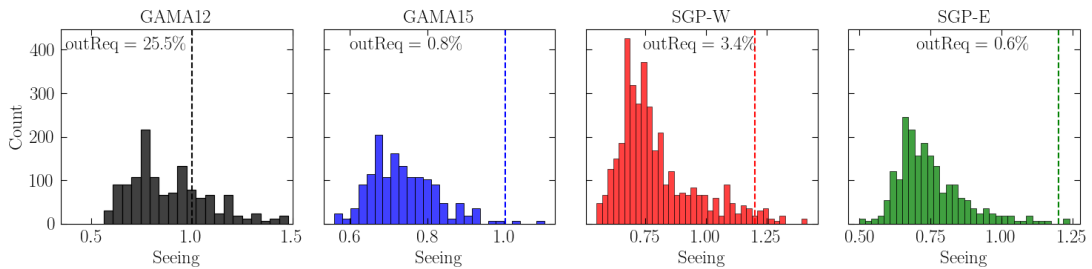


Figure 2: Seeing distribution for all normal images being part of the DR1 release in each field separately. Apart from the GAMA-12h field, where 25% of the images exceed the seeing requirement, most images are fulfilling the observing requirements. In the case of GAMA-12h, these images come from adjacent tiles used to fill-up to the edges.

In Fig. 2, we show the distribution of the average seeing for all normal images entering the DR1 data in each field. In Fig. 3 we show the distribution of airmass.

The two tiles in the G12 field have an unexpectedly large proportion of normal images exceeding the observing requirements. These images come from adjacent tiles used to fill-up to the edges. In Fig. 4 we show the footprint of the 10 mosaics for the G12 (top), G15 (middle) and SGP (bottom) fields and in Table 1 we summarize the main properties of them.

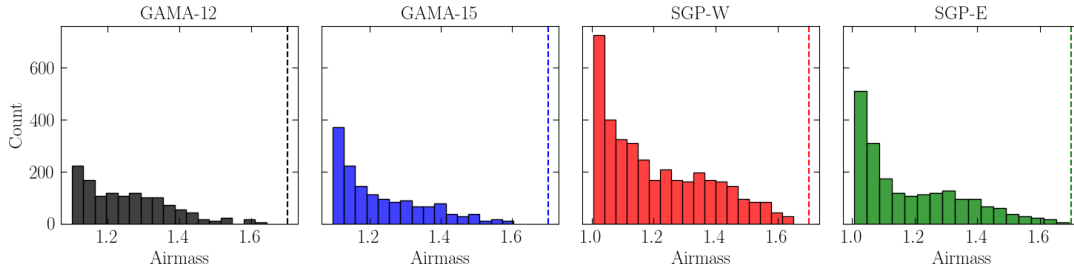


Figure 3: Airmass distribution for all images entering the DR1 release in each field separately. All meet the requirement of airmass < 1.7.

## Release Content

SHARKS-DR1 consists of 10 co-added images and individual  $K_s$ -band source catalogues. This data release includes:

- calibrated co-added images, astrometrically and photometrically calibrated with respect to 2MASS
- normalized weight images
- calibrated source catalogues
- preimage (jpg file) related to each (weight) image

Other value-added products will be found at:

<http://research.iac.es/proyecto/sharks/pages/en/data-releases/dr1.php>

DR1 images are distributed over the three SHARKS fields, where six of them are isolated and four of them cover a contiguous region in the SGP-E field. The total area of each mosaic is 2.03 square degrees. In the four contiguous pointings in the SGP-E field, there is an overlap of 1.03 square degrees (13%) within the tiles, completing 7.06 square degrees. In total, the unique area of DR1 is 19.24 square degrees, 20.27 square degrees considering the overlap.

Images were co-added using *SWarp* (Bertin E., 2010, ASPC, 281, 228) and catalogues are obtained using *SExtractor* (Bertin, E., 1996, A&AS, 117, 393)<sup>2</sup>. Data processing has been tuned to detect the faintest sources. The average  $5\sigma$  magnitude limit (AB) for point sources in the catalogue is 22.65 mag, with an average standard deviation of  $\sim 0.25$  mag over the footprint. In the SGP-E region, since images overlap and catalogues are distributed tile-by-tile, there will be duplications. The total DR1 data size is 3.5 Gb, including images and catalogues. Images are compressed using the "RICE" compression method. Images and catalogues are available at ESO<sup>3</sup> and IAC services<sup>4</sup>.

<sup>2</sup> <https://www.astromatic.net/>

<sup>3</sup> <http://archive.eso.org/cms.html>

<sup>4</sup> <http://research.iac.es/proyecto/sharks/pages/en/data-releases/dr1.php>

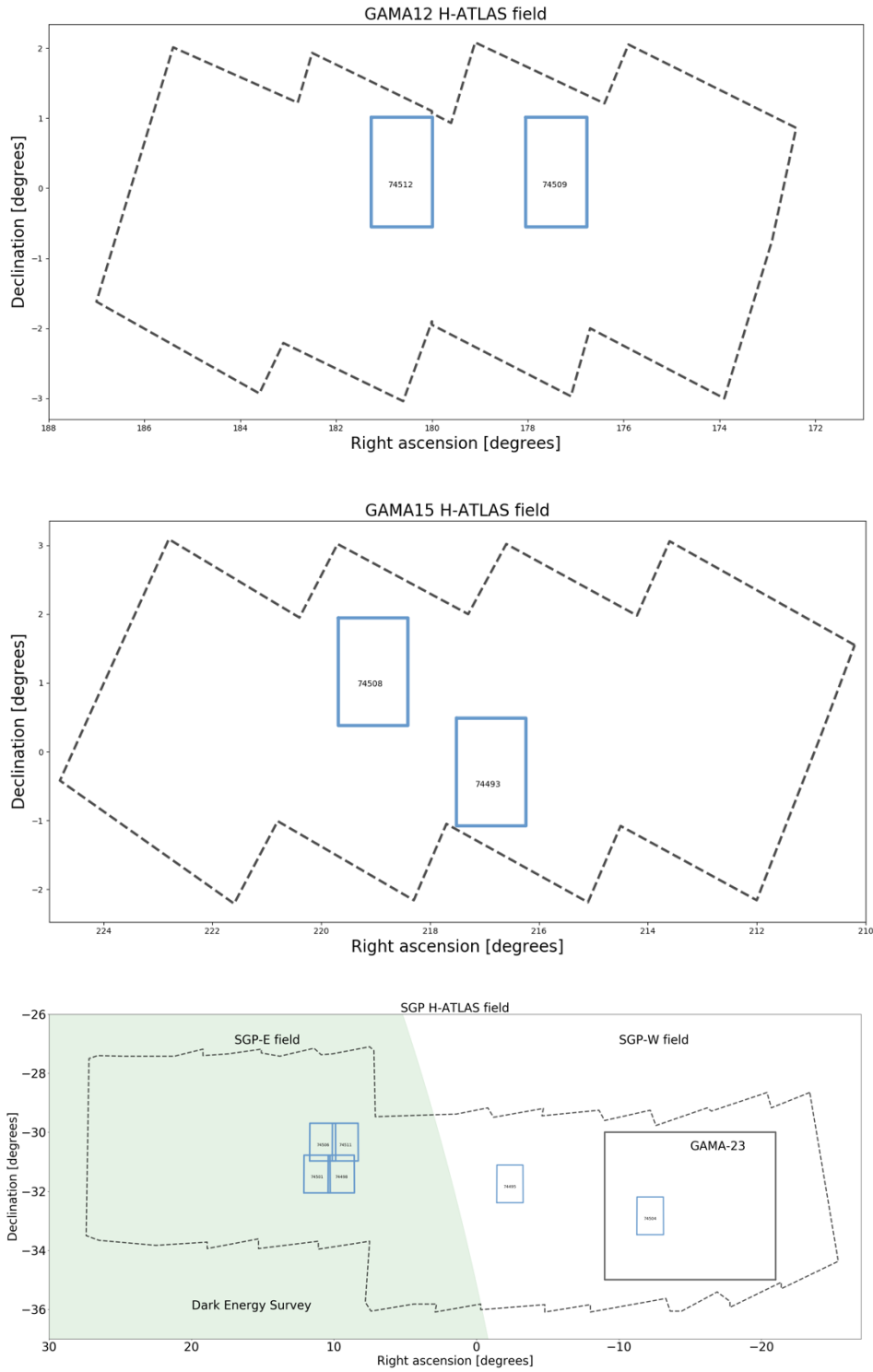


Figure 4: SHARKS-DR1 spatial distribution for the 10 SHARKS-DR1 tiles (in blue). In dashed, the H-ATLAS<sup>5</sup> footprint of the G12 (upper panel), G15 (middle panel) and SGP field (bottom panel). For the SGP region, we further show the GAMA-23h footprint (in black) and the Dark Energy Survey<sup>6</sup> one (filled green).

<sup>5</sup> <https://www.h-atlas.org/>

<sup>6</sup> <https://www.darkenergysurvey.org/>

Table 1: Summary of the 10 SHARKS-DR1 mosaics

ImageID <sup>7</sup>	RA (J2000)	Dec (J2000)	FWHM (arcsec)	Depth $5\sigma$ (mag in AB)	Sources
<b>GAMA-12h</b> Area = 4.06 deg <sup>2</sup> Density = 20.25 sources/arcmin <sup>2</sup>					
74509	11h49m38.029s	00d13m44.37s	1.01	22.54	153492
74512	12h02m30.658s	00d13m50.84s	1.04	22.41	142413
<b>GAMA-15h</b> Area = 4.06 deg <sup>2</sup> Density = 23.18 sources/arcmin <sup>2</sup>					
74493	14h27m30.544s	-00d17m47.24s	1.00	22.51	166305
74508	14h36m11.747s	01d09m45.19s	1.02	22.59	172550
<b>SGP-W</b> Area = 4.06 deg <sup>2</sup> Density = 23.69 sources/arcmin <sup>2</sup>					
74504	23h11m13.428s	-32d50m02.00s	1.02	22.62	162340
74495	23h50m36.622s	-31d45m08.91s	1.03	22.72	183966
<b>SGP-E<sup>8</sup></b> Area = 7.06 deg <sup>2</sup> Density = 24.48 sources/arcmin <sup>2</sup>					
74501	0h44m46.575s	-31d25m04.83s	1.00	22.77	171520
74498	0h37m57.484s	-31d24m54.91s	1.00	22.85	194292
74511	0h36m50.029s	-30d20m03.93s	1.00	22.82	189558
74506	0h43m10.876s	-30d19m58.59s	1.03	22.70	160270

## Release Notes

This is the first data release of the SHARKS survey. Images are reduced and calibrated at the WFAU and with a new sky-background subtraction algorithm, developed in collaboration between the IAC and WFAU. In the process, we use products from the Cambridge Astronomy Survey Unit (CASU), in particular, we use the astrometric and photometric calibrations tightened to 2MASS. We note that the VISTA Data Flow System pipeline processing and science archive are

<sup>7</sup> The ImageID starts with "10000000" followed by the number given in this column.

<sup>8</sup> The given area for SGP-E takes into account the overlapping regions whereas the density of sources is based on the area covered by each field.

described in Irwin et al (2004, SPIE, 5493, 411), Hambly et al (2008, MNRAS, 384, 637) and Cross et al. (2012, A&A, 548, 119).

The pipeline starts by retrieving CASU processed normals and stacked pawprints (first reduced with the “tilesky” method). The image reduction is done in three steps: 1) new sky-subtracted normals are computed, 2) next, stacked pawprints are re-created and resampled and 3) deep mosaics are made from these new stacked pawprints. We use a combination of Python scripts and the *SWarp* code (v2.38). To form the co-addition, mosaic images are resampled to a pixel size of  $\sim 0.34$  arcsec at the image center using wcs tangential (TAN) projection, pixel units are given in ADU. Weight images are normalized to effective gains (in ADU).

Images are astrometrically and photometrically calibrated with respect to 2MASS (Skrutskie et al. 2006, AJ, 131, 1163). Details about the calibration can be found in González-Fernández et al. 2018 (MNRAS, 474, 5459).

Source catalogues are obtained with the *SExtractor* code (v2.19.5). Photometry is given in the AB system and we have calculated aperture corrections for 13 standard apertures, from 1'' to 24'' (see Table 5 in Section 4.5). For extended sources we have Kron and Petrosian fluxes, which account for much of the missing light.

## Data Reduction and Calibration

As already mentioned, data has been reduced at WFAU with an alternative sky-background subtraction method. In this method, we calculate one sky-background image for each single-epoch image (normal frames, 36 per OB), instead of one single sky-background image per OB (the so-called “tilesky” method at CASU). Next, with the new sky-subtracted normal images, we re-create new stacked pawprints (six per OB) and finally stacked pawprints from all OBs are co-added into the mosaic. In SHARKS-DR1, in order to make the co-added mosaic, we use any stacked pawprints that overlap with the given mosaic footprint. These pawprints are reduced in the same manner.

### Normal re-creation

We first create sky-backgrounds for each normal frame, based on a running sky-subtraction algorithm, and correct them. We nonetheless make use of the normal frames and stacked pawprint images reduced at CASU, which have been corrected for<sup>9</sup>: reset, dark, linearity, flat field, sky-background and stripe correction.

In order to re-create the new sky-subtracted normals, we apply the following algorithm:

1. We run *SExtractor* on each stacked pawprint in order to create segmentation images. These images will be used to mask sources in the normal frames when we estimate the median sky for each normal.
2. For each normal, we add back the OB sky background image, created with the “tilesky” algorithm.

---

<sup>9</sup> <http://casu.ast.cam.ac.uk/surveys-projects/vista/technical/data-processing>

3. Next, we calculate a sky image for each normal frame as the median of all normals (masked with the segmentation images produced before), that have been observed in a time window. For a given normal, we median the sky in a time window of 14 minutes, i.e.: with normals taken seven minutes before and after. If an image has been taken before seven minutes of the start of the OB, or after seven minutes before the end of the OB, then we extend the time windows to ten minutes to have a number of images similar for all normals in the OB. This way, we end up with 36 sky images per OB, one per normal frame.
4. Finally, the sky image is subtracted from the normal frame to obtain the alternative, sky-background subtracted normals.

### Stacked pawprint re-creation

Sky-subtracted normals are then stacked to make new stacked pawprints. This stage is done using the *SWarp* code. Images are resampled using a bilinear interpolation including oversampling. Also, at this stage we resample to the final pixel size and change coordinate projections to Gnomonic projection (TAN). It is important to say that the bilinear interpolation degrades the image quality by  $\sim 15\%$ , which effectively worsens the effective seeing of our images. Nonetheless, our tests show that we are able to detect sources 0.5 magnitudes fainter with this interpolation. Future releases will improve over this decision. No further sky-subtraction is done at this step. The *SWarp* configurations used in this step is shown in Table 2.

Table 2: *SWarp* parameters used to recreate the stacked pawprints

RESCALE_WEIGHTS	Y
COMBINE_TYPE	CLIPPED
CLIP_AMPFRAC	0.3
CLIP_SIGMA	2.0
BLANK_BADPIXELS	N
PROJECTION_TYPE	TAN
PROJECTION_ERR	0.0
PIXELSCALE_TYPE	MANUAL
IMAGE_SIZE	AUTOMATIC
RESAMPLING_TYPE	BILINEAR
OVERSAMPLING	3,3
INTERPOLATE	N
FSCALASTRO_TYPE	FIXED
GAIN_KEYWORD	GAINCOR
SUBTRACT_BACK	N

### Deep mosaic co-addition

Finally, we co-add together all stacked pawprints for all OBs overlapping the footprint of the mosaic. Again, we use *SWarp* for the co-addition. At this stage, we apply further internal sky-subtraction. The configuration is shown in Table 3.

Table 3: *SWarp* parameters used to create the final deep mosaic

RESCALE_WEIGHTS	Y
COMBINE_TYPE	CLIPPED
CLIP_AMPFRAC	0.3
CLIP_SIGMA	3.0
PROJECTION_TYPE	TAN
PROJECTION_ERR	0
PIXEL_SCALE	0.34
IMAGE_SIZE	Automatic
RESAMPLING_TYPE	LANCZOS3
OVERSAMPLING	automatic
INTERPOLATE	N
FSCALASTRO_TYPE	VARIABLE
GAIN_KEYWORD	GAIN
SUBTRACT_BACK	Y
BACK_TYPE	AUTO
BACK_SIZE	32
BACK_FILTERSIZE	3
BACK_FILTTHRESH	0.0

Each mosaic is then photometrically calibrated with respect to 2MASS in the AB magnitude system and the zeropoint is updated to each image header. To do so, we run *SExtractor* a first time and match the sources in our mosaic to sources in the CASU system (already calibrated).

### Source extraction

We use *SExtractor* to produce the catalogues separately from the calibrated images. The configuration parameters are shown in Table 4. We calculate magnitudes for 13 different apertures listed in Table 5. The full list of columns can be found in Section 8.2.



Table 4: *SExtractor* parameters used to extract the mosaic catalogues

DETECT_MINAREA	9
DETECT_THRESH	1.1
ANALYSIS_THRESH	2.
THRESH_TYPE	RELATIVE
FILTER	Y
FILTER_NAME	gauss_3.0_5x5.conv
DEBLEND_NTHRESH	64
DEBLEND_MINCONT	0.0007
CLEAN	Y
CLEAN_PARAM	1
MASK_TYPE	CORRECT
PHOT_APERTURES	<i>See below</i>
PHOT_FLUXFRAC	0.2, 0.5, 0.8
PHOT_AUTOPARAMS	2.0, 3.3
PHOT_AUTOAPERS	15.0, 15.0
PHOT_PETROPARAMS	2.0,3.3
SATUR_KEY	SATURATE
GAIN_KEY	GAIN
SEEING_FWHM	1.
STARNNW_NAME	default.nnw
BACK_SIZE	64
BACK_FILTERSIZE	3
BACKPHOTO_TYPE	LOCAL
BACKPHOTO_THICK	24
BACK_TYPE	AUTO

Further notes on the catalogue extraction:

- Magnitudes are not corrected for extinction. In the  $K_s$ -band, the effect is expected to be small. Nonetheless, we recommend a zero-point correction for extragalactic sources as:  $K_{s,\text{corrected}} = K_s - 0.005 * E(B-V)$ , where  $E(B-V)$  is preferable from the SFD98 map (Schlegel et al. 1998, ApJ. 500, 2).

- $K_s$  transformation to Vega is  $\sim -1.827$  mag ( $K_{s,Vega} = K_{s,AB} - 1.827$ ).
- In this release, no illumination correction has been applied since this effect is negligible in the  $K_s$  band.

## Data Quality

### Astrometry

SHARKS-DR1 is astrometrically calibrated with respect to 2MASS in the J2000 epoch. We plan to include astrometric solutions with respect to Gaia<sup>10</sup> for future SHARKS data releases, but for SHARKS-DR1 we directly use the calibrations given by CASU. In order to validate the astrometric quality of our images, we run *SCAMP* (v2.9.2; Bertin, 2006, ASPC, 351, 112) to obtain metrics for each mosaic separately with respect to 2MASS. On average, 2500 stars are found in each mosaic. The mean astrometric offset is compatible with zero, within an uncertainty of  $\pm 0.2''$ , smaller than the pixel size of our images. Likewise, image distortions are within 0.01% through the mosaic area. In Fig. 5 we show the *SCAMP* result for a mosaic as an example. All individual mosaic results are in <http://research.iac.es/proyecto/sharks/pages/en/data-releases/dr1/validation.php>.

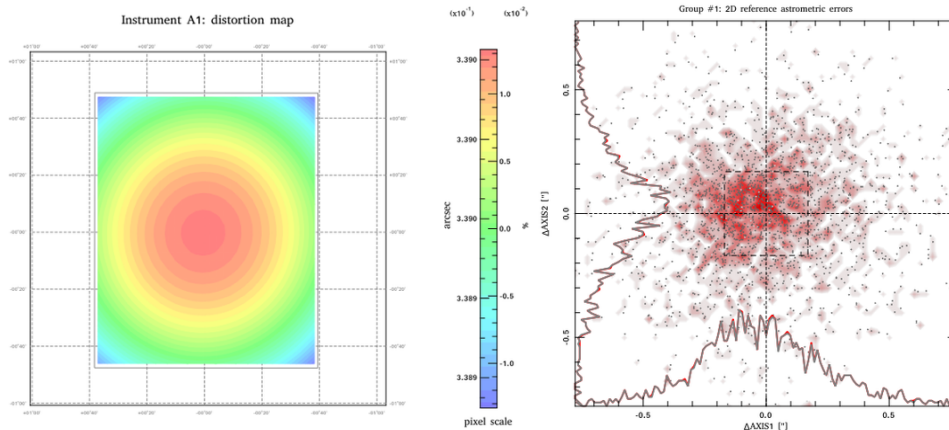


Figure 5: Example of *SCAMP* result metrics for mosaic with *imageID* = 74509. On the left, astrometric distortion. On the right, astrometric difference with respect to 2MASS stars.

We further test the astrometric homogeneity in the SGP-E contiguous area. We plot the mean astrometric separation in each *healpix* pixels of NSIDE=512 between SHARKS and 2MASS stars (within 1 arcsec). There are  $\sim 16$  stars per *healpix* pixel to obtain the mean separation. No systematic patterns are found apart from some small regions in the borders, where the sampling is less homogeneous (see Fig. 6).

### Photometry

Photometry is also calibrated with respect to 2MASS using the CASU calibrated products. In order to evaluate the homogeneity of SHARKS photometry, we compare the magnitudes in the SHARKS catalogue with respect to the VIKING DR4

<sup>10</sup> <https://www.cosmos.esa.int/web/gaia/home>

data<sup>11</sup>. For clarity, we only show results from the contiguous SGP-E region, but conclusions apply to all fields.

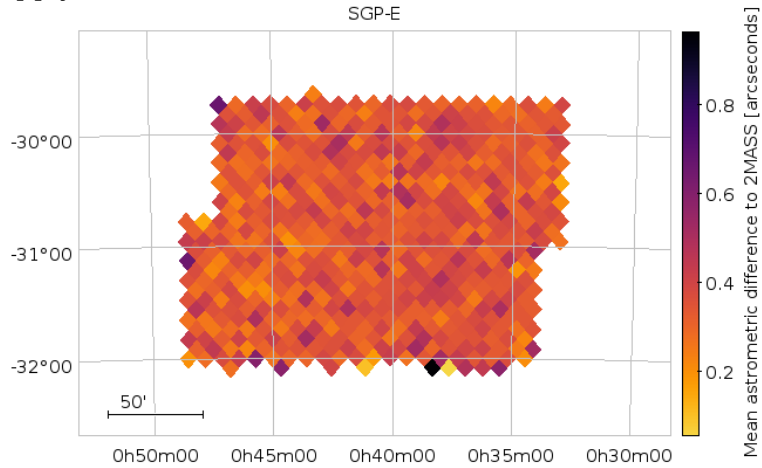


*Fig. 6: Mean absolute astrometric difference between SHARKS and 2MASS stars in the SGP-E field in arcseconds. No pathological patterns are found, apart from some regions in the borders with high astrometric differences.*

We first match SHARKS sources to VIKING within  $1''$  radius. In the SGP-E region, this results in  $\sim 190,000$  matches, including both stars and galaxies. Next, we pixelize the matched catalogue using *healpix* (NSIDE=2048, resolution of 2.95 arcminutes) and estimate the mean photometric offset in each pixel ( $K_s$  SHARKS -  $K_s$  VIKING). In both cases we use petrosian magnitudes and do not separate between point and extended sources. We find a good agreement between SHARKS and VIKING, with a standard deviation of  $\sim 0.1$  and no clear structures in the footprint. Results are shown in Fig. 7.

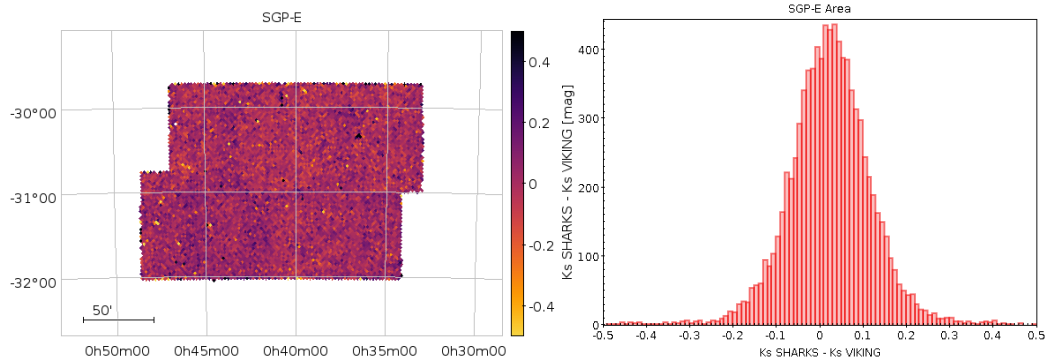


*Fig. 7: Mean difference between SHARKS and VIKING magnitudes ( $K_s$  SHARKS -  $K_s$  VIKING) for all sources in the SGP-E field, using petrosian magnitudes in the AB system. Larger differences are associated with bright stars and diffraction spikes.*

### Image quality

We run *PSFEx* (v3.21.1; Bertin, 2011, ASPC, 442, 435) to study the image quality. As already noted, the effective seeing is around  $1''$ , even though the average seeing is better than that. This highlights a degradation of the image quality coming from the image reduction process of up to 15%. In fact, most of the image degra-

<sup>11</sup> <https://www.eso.org/sci/publications/announcements/sciann17289.html>

dition comes from the bilinear interpolation applied during the stacked pawprint re-creation. On the other hand, this interpolation improves over the depth. For SHARKS-DR1, we have prioritized completeness over purity and image quality.

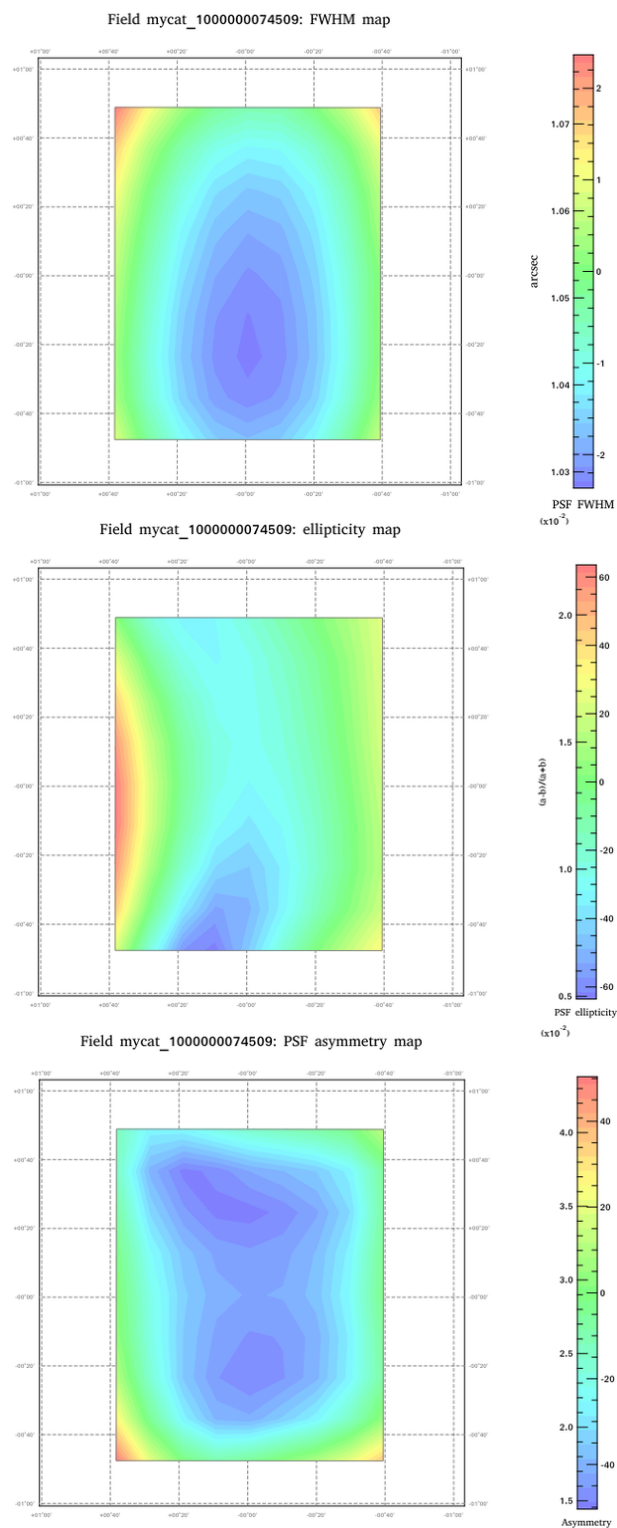


Figure 8: PSFEx metrics for one mosaic as an example (*imageID* = 74509). On the top, FWHM distribution, on the middle, ellipticity distribution and on the bottom, PSF asymmetry distribution.

After running *PSFEx*, we detect PSF distortions that vary from tile to tile, with maximum variations of 5% to more homogeneous PSF profiles with 2% variation. Ellipticity is always below 0.02 (defined as  $a-b/a+b$ ). As with *SCAMP* solutions, we do not correct for PSF variations in SHARKS-DR1.

In Fig. 8 we show an example of *PSFEx* metrics for one mosaic. Results for all mosaics can be found in:

<http://research.iac.es/proyecto/sharks/pages/en/data-releases/dr1/validation.php>

### Depth

We estimate the magnitude limit distribution at  $5\sigma$  for a  $2''$  aperture in a  $100\times 100$  grid in each mosaic image. To estimate the image depth in each point in the grid, we exclude the contribution of pixels coming from sources detected in the images. We do this by masking the image with the segmentation image produced by *SExtractor*. Results are shown in Fig. 9 for one example. Please visit <http://research.iac.es/proyecto/sharks/pages/en/data-releases/dr1/validation.php> for all results.

Furthermore, we estimate the depth of each image by measuring the average magnitude for sources with a magnitude significance of  $5\sigma$  (magnitude error of  $\sim 0.217$ ). This second estimate is the one given in Table 1 and in the image headers. The agreement between both estimates is within  $1\sigma$  of the standard deviation.

With the former estimate, we estimate how homogeneous the depth is. As expected by design, we can see the detectors overlapping regions (see Fig. 9), where we nominally have more exposures per pixel and therefore a greater depth. Calculating the standard deviation of the depth in each mosaic, we get an average deviation of  $\sim 0.16$  mag in  $5\sigma$  depth.

### Spurious sources and artifacts

Bright stars, extended galaxies and other imaging artifacts are not particularly treated in the images. No treatment is done at the catalogue level either, although the column `ERRBITS`<sup>12</sup> maps spurious sources in the borders and around bright stars. Nonetheless, we expect a low number of spurious sources and artifacts associated with these issues.

### Known issues

Next, we list known issues for SHARKS-DR1. As this list increases, we will keep an updated version on: <http://research.iac.es/proyecto/sharks/pages/en/data-releases/dr1/knownissues.php>

- Bright stars and other imaging artifacts are not removed, neither masked in this release. We roughly estimate the contribution of these sources to less than 1% of the catalogue.

---

<sup>12</sup> *SExtractor* flag as described in <https://sextractor.readthedocs.io/en/latest/Flagging.html#extraction-flags-flags>

- There are duplications at the overlapping mosaics in the SGP-E field.
- Current bilinear interpolation degrades the image PSF by  $<15\%$ , but depth sensibility increases by 0.5 magnitudes.

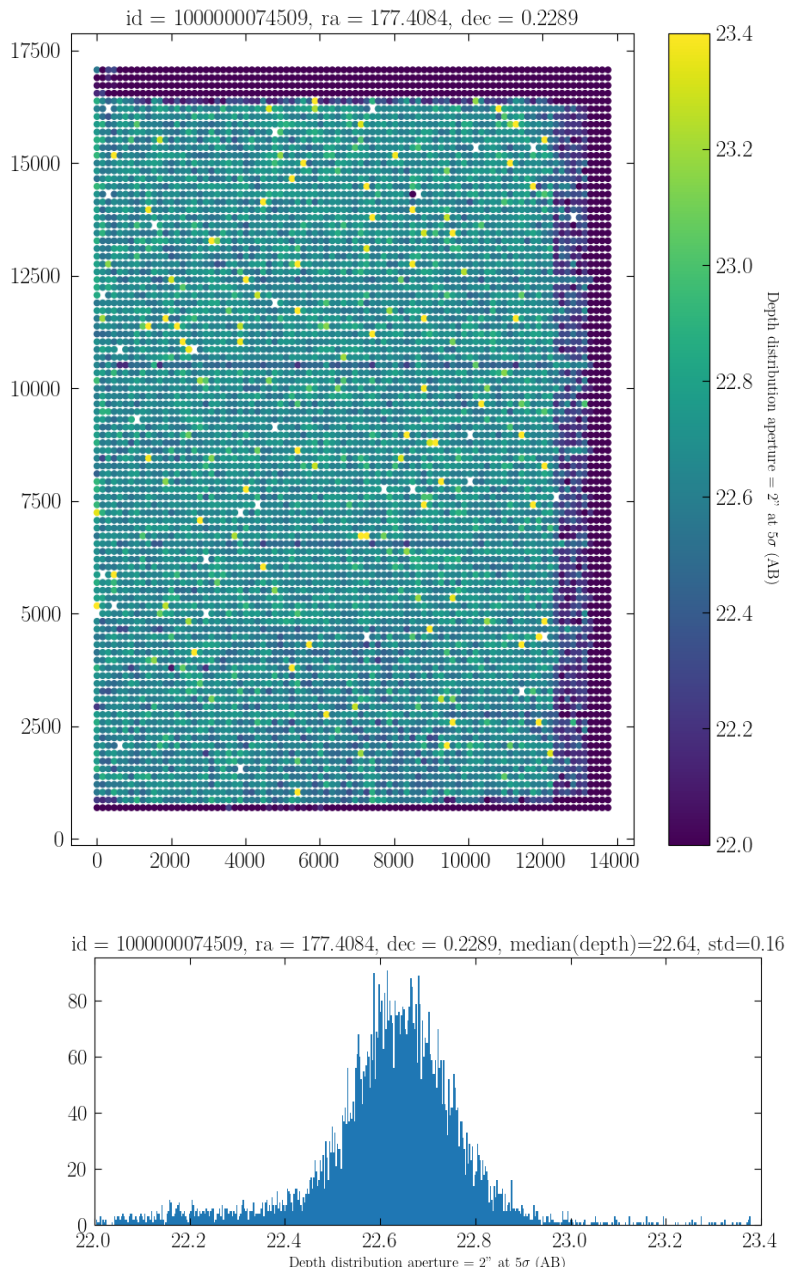


Figure 9: Depth distribution for  $5\sigma$ , calculated in a  $2''$  aperture (AB) after considering the given sky noise and exposure times. At the top, depth distribution as a function of position. At the bottom, histogram of the distribution. This is one example (imageID = 74509). For all mosaics, visit the IAC SHARKS-DR1 webpage.

## Previous Releases

This is the first data release of SHARKS.

## Data Format

### Files Types

This release is made of three types of files per mosaic, all in fits format. Images are further compressed using the Rice compression method. The file naming convention is the following (everything within <> change from mosaic to mosaic):

**Source catalogues:** sharks\_dr1\_<RADEC>\_mosaic\_ks\_cat\_<ImageID>.fits

**Image:** sharks\_dr1\_<RADEC>\_mosaic\_ks\_deepimage\_<ImageID>.fits.fz

**Weight Image:** sharks\_dr1\_<RADEC>\_mosaic\_ks\_deepconf\_<WeightID>.fits.fz

In addition, related to each (weight) image we provide a jpg file.

Table 5: *Parameters related to the file name*

<RADEC>	<ImageID>	<WeightID>
00h36-30d20	1000000074511	1000000074503
00h37-31d24	1000000074498	1000000074496
00h43-30d19	1000000074506	1000000074497
00h44-31d25	1000000074501	1000000074502
11h49+00d13	1000000074509	1000000074505
12h02+00d13	1000000074512	1000000074494
14h27-00d17	1000000074493	1000000074500
14h36+01d09	1000000074508	1000000074507
23h11-32d50	1000000074504	1000000074510
23h50-31d45	1000000074495	1000000074499

### Catalogue Columns

Table 6: *Name, description and units of the catalogue columns*

Column name	Description	Units
MULTIFRAMEID	the UID of the relevant multiframe	
EXTNUM	the extension number of this frame	
CUEVENTID	UID of curation event giving rise to this record	

SEQNUM	the running number of this detection	
FILTERID	UID of combined filter (5=Ks)	
ISOFLUX	Instrumental isophotal flux counts (SE: FLUX_ISO)	ADU
ISOMAG	Calibrated isophotal magnitude	mag
X	X coordinate of detection (SE: X_IMAGE)	pix
XERR	Error in X coordinate (SE: ERRX2_IMAGE)	pix
Y	Y coordinate of detection (SE: Y_IMAGE)	pix
YERR	Error in Y coordinate (SE: ERRY2_IMAGE)	pix
GAUSIG	RMS of axes of ellipse fit	pix
ELL	$1-b/a$ , where $a/b$ =semi-major/minor axes (SE: THE-TA_IMAGE)	
PA	ellipse fit orientation to x axis	deg
APROF1	Isophotal area at level 0 (analysis threshold) (SE: ISO0)	pixel
APROF2	Isophotal area at level 1 (analysis threshold) (SE: ISO1)	pixel
APROF3	Isophotal area at level 2 (analysis threshold) (SE: ISO2)	pixel
APROF4	Isophotal area at level 3 (analysis threshold) (SE: ISO3)	pixel
APROF5	Isophotal area at level 4 (analysis threshold) (SE: ISO4)	pixel
APROF6	Isophotal area at level 5 (analysis threshold) (SE: ISO5)	pixel
APROF7	Isophotal area at level 6 (analysis threshold) (SE: ISO6)	pixel
APROF8	Isophotal area at level 7 (analysis threshold) (SE: ISO7)	pixel
PHEIGHT	Highest pixel value above sky (SE: FLUX_MAX)	ADU
PHEIGHTERR	Error in peak height	ADU
APERFLUX1	Default aperture flux counts 1, no aperture correction applied	ADU
APERFLUX1ERR	Error in aperture flux counts 1 (SE: FLUXERR_APER1)	ADU
APERMAGNOAPERCORR1	As aperMag1 but no aperture correction applied	mag
APERMAG1	Calibrated and corrected aperture magnitude 1	mag
APERMAG1ERR	Error in calibrated aperture magnitude 1	mag
APERFLUX2	Default aperture flux counts 2, no aperture correction applied	ADU
APERFLUX2ERR	Error in aperture flux counts 2 (SE: FLUXERR_APER2)	ADU
APERMAGNOAPERCORR2	As aperMag2 but no aperture correction applied	mag



APERMAG2	Calibrated and corrected aperture magnitude 2	mag
APERMAG2ERR	Error in calibrated aperture magnitude 2	mag
APERFLUX3	Default aperture flux counts 3, no aperture correction applied	ADU
APERFLUX3ERR	Error in aperture flux counts 3 (SE: FLUXERR_APER3)	ADU
APERMAGNOAPERCORR3	As aperMag3 but no aperture correction applied	mag
APERMAG3	Calibrated and corrected aperture magnitude 3	mag
APERMAG3ERR	Error in calibrated aperture magnitude 3	mag
APERFLUX4	Default aperture flux counts 4, no aperture correction applied	ADU
APERFLUX4ERR	Error in aperture flux counts 4 (SE: FLUXERR_APER4)	ADU
APERMAGNOAPERCORR4	As aperMag4 but no aperture correction applied	mag
APERMAG4	Calibrated and corrected aperture magnitude 4	mag
APERMAG4ERR	Error in calibrated aperture magnitude 4	mag
APERFLUX5	Default aperture flux counts 5, no aperture correction applied	ADU
APERFLUX5ERR	Error in aperture flux counts 5 (SE: FLUXERR_APER5)	ADU
APERMAGNOAPERCORR5	As aperMag5 but no aperture correction applied	mag
APERMAG5	Calibrated and corrected aperture magnitude 5	mag
APERMAG5ERR	Error in calibrated aperture magnitude 5	mag
APERFLUX6	Default aperture flux counts 6, no aperture correction applied	ADU
APERFLUX6ERR	Error in aperture flux counts 6 (SE: FLUXERR_APER6)	ADU
APERMAGNOAPERCORR6	As aperMag6 but no aperture correction applied	mag
APERMAG6	Calibrated and corrected aperture magnitude 6	mag
APERMAG6ERR	Error in calibrated aperture magnitude 6	mag
APERFLUX7	Default aperture flux counts 7, no aperture correction applied	ADU
APERFLUX7ERR	Error in aperture flux counts 7 (SE: FLUXERR_APER7)	ADU
APERMAGNOAPERCORR7	As aperMag7 but no aperture correction applied	mag
APERMAG7	Calibrated and corrected aperture magnitude 7	mag
APERMAG7ERR	Error in calibrated aperture magnitude 7	mag
APERFLUX8	Default aperture flux counts 8, no aperture correction	ADU

	applied	
APERFLUX8ERR	Error in aperture flux counts 8 (SE: FLUXERR_APER8)	ADU
APERMAGNOAPERCORR8	As aperMag8 but no aperture correction applied	mag
APERMAG8	Calibrated and corrected aperture magnitude 8	mag
APERMAG8ERR	Error in calibrated aperture magnitude 8	mag
APERFLUX9	Default aperture flux counts 9, no aperture correction applied	ADU
APERFLUX9ERR	Error in aperture flux counts 9 (SE: FLUXERR_APER9)	ADU
APERMAGNOAPERCORR9	As aperMag9 but no aperture correction applied	mag
APERMAG9	Calibrated and corrected aperture magnitude 9	mag
APERMAG9ERR	Error in calibrated aperture magnitude 9	mag
APERFLUX10	Default aperture flux counts 10, no aperture correction applied	ADU
APERFLUX10ERR	Error in aperture flux counts 10 (SE: FLUXERR_APER10)	ADU
APERMAGNOAPERCORR10	As aperMag10 but no aperture correction applied	mag
APERMAG10	Calibrated and corrected aperture magnitude 10	mag
APERMAG10ERR	Error in calibrated aperture magnitude 10	mag
APERFLUX11	Default aperture flux counts 11, no aperture correction applied	ADU
APERFLUX11ERR	Error in aperture flux counts 11 (SE: FLUXERR_APER11)	ADU
APERMAGNOAPERCORR11	As aperMag11 but no aperture correction applied	mag
APERMAG11	Calibrated and corrected aperture magnitude 11	mag
APERMAG11ERR	Error in calibrated aperture magnitude 11	mag
APERFLUX12	Default aperture flux counts 12, no aperture correction applied	ADU
APERFLUX12ERR	Error in aperture flux counts 12 (SE: FLUXERR_APER12)	ADU
APERMAGNOAPERCORR12	As aperMag12 but no aperture correction applied	mag
APERMAG12	Calibrated and corrected aperture magnitude 12	mag
APERMAG12ERR	Error in calibrated aperture magnitude 12	mag
APERFLUX13	Default aperture flux counts 13, no aperture correction applied	ADU

APERFLUX13ERR	Error in aperture flux counts 13 (SE: FLUXERR_APER13)	ADU
APERMAGNOAPERCORR13	As aperMag13 but no aperture correction applied	mag
APERMAG13	Calibrated and corrected aperture magnitude 13	mag
APERMAG13ERR	Error in calibrated aperture magnitude 13	mag
PETRORAD	Petrosian radius (SE: PETRO_RADIUS*A_IMAGE)	pix
KRONRAD	Kron radius as defined in SE by Graham and Driver (2005)	pix
HALFRAD	SExtractor half-light radius (FRAC_RADIUS)	pix
HLCIRCRADAS	Circular half-light radius computed from curve of growth	arcsec
HLCIRCRADERRAS	Error in hlCircRadAs	arcsec
HLGEORADAS	Geometric half-light radius	arcsec
HLSMNRADAS	Half-light semi-minor axis	arcsec
HLSMJRADAS	Half-light semi-major axis	arcsec
HLCORSMNRADAS	Seeing corrected Half-light semi-minor axis	arcsec
HLCORSMJRADAS	Seeing corrected Half-light semi-major axis	arcsec
PETROFLUX	flux within Petrosian radius circular aperture (SE: FLUX_PETRO)	ADU
PETROFLUXERR	error on Petrosian flux (SE: FLUXERR_PETRO)	ADU
PETROMAG	Calibrated Petrosian magnitude within circular aperture r_p	mag
PETROMAGERR	error on calibrated Petrosian magnitude	mag
KRONFLUX	flux within Kron radius circular aperture (SE: FLUX_AUTO)	ADU
KRONFLUXERR	error on Kron flux (SE: FLUXERR_AUTO)	ADU
KRONMAG	Calibrated Kron magnitude within circular aperture r_k	mag
KRONMAGERR	error on calibrated Kron magnitude	mag
HALFFLUX	Half the total flux (max(isoFlux,aperFlux5))	ADU
HALFFLUXERR	error on Half flux, not available in SE output	ADU
HALFMAG	Calibrated magnitude within circular aperture halfRad	mag
HALFMAGERR	Calibrated error on Half magnitude, not available in SE output	mag
ERRBITS	processing warning/error bitwise flags	

SKY	local interpolated sky level from background tracker	ADU
SKYVAR	local estimate of variation in sky level around image	ADU
AVERAGECONF	Average confidence level in default 2 arcsec diameter aperture 3	
MJD	The mean Modified Julian Day of each detection	day
RA	Celestial Right Ascension	deg
DEC	Celestial Declination	deg
L	Galactic longitude	deg
B	Galactic latitude	deg
LAMBDA	SDSS system spherical co-ordinate 1	deg
ETA	SDSS system spherical co-ordinate 2	deg
CLASS	Flag indicating most probable morphological classification	
CLASSSTAT	S-Extractor classification statistic CLASS_STAR (0-galaxy,1-star)	
PSFFLUX	Not available	
PSFFLUXERR	Not available	
PSFMAG	Not available	
PSFMAGERR	Not available	
PSFFITX	Not available	
PSFFITXERR	Not available	
PSFFITY	Not available	
PSFFITYERR	Not available	
PSFFITCHI2	Not available	
PSFFITDOF	Not available	
SERFLUX1D	Not available	
SERMAG1D	Not available	
SERSCALELEN1D	Not available	
SERIDX1D	Not available	
SERFIT1DCHI2	Not available	
SERFITNU1D	Not available	
SERFLUX2D	Not available	

SERMAG2D	Not available	
SERSCALELEN2D	Not available	
SERIDX2D	Not available	
SERFIT2DCHI2	Not available	
SERFITNU2D	Not available	
DELTAMAG	sum of magnitude corrections for faster processing	
ILLUMCORR	illumination correction. = 0	
DISTORTCORR	distortion correction. = 0	
SATURATCORR	saturation correction. = 0	
PPERBITS	Not available	
DEPRECATED	Not available	
OBJID	Unique identifier for this detection or default for no de- tection	

## Acknowledgements

*Any publication making use of this data, whether obtained from the ESO archive or via third parties, must include the following acknowledgements:*

- "Based on data products created from observations collected at the European Organisation for Astronomical Research in the Southern Hemisphere under ESO programme 198.A-2006."
- "For the creation of the data used in this work, the SHARKS team at the Instituto de Astrofísica de Canarias has been financial supported by the Spanish Ministry of Science, Innovation and Universities (MICIU) under grant AYA2017-84061-P, co-financed by FEDER (European Regional Development Funds), by the Spanish Space Research Program "Participation in the NISP instrument and preparation for the science of EUCLID" (ESP2017-84272-C2-1-R) and by the ACIISI, Consejería de Economía, Conocimiento y Empleo del Gobierno de Canarias and the European Regional Development Fund (ERDF) under grant with reference PROID2020010107."
- "We thank the support of the Wide-Field Astronomy Unit for testing and parallelising the mosaic process and preparing the releases. The work of the Wide-Field Astronomy Unit is funded by the UK Science and Technology Facilities Council through grant ST/T002956/1."

*If the access to the ESO Science Archive Facility services was helpful for your research, please include the following acknowledgment:*

- "This research has made use of the services of the ESO Science Archive Facility."

*Science data products from the ESO archive may be distributed by third parties, and disseminated via other services, according to the terms of the [Creative Commons Attribution 4.0 International license](#). Credit to the ESO origin of the data must be acknowledged, and the file headers preserved.*

## **Version**

- Version 1.0 published on 31 January 2022.